Long term behaviour based on a weakness planes approach: Constitutive model and application to a Meuse/Haute-Marne (France) URL drift

Mountaka Souley
National Institute for Industrial Environment and Risks (Ineris), Nancy, France

Minh-Ngoc Vu
Radioactive Waste Management Agency (Andra), Chatenay-Malabry, France

Gilles Armand
Radioactive Waste Management Agency (Andra), Bure, France

ABSTRACT: A constitutive model considering the natural and induced anisotropies in the short- and long-term behaviour is proposed by combining the elasto-visco-plasticity for rock matrix and weakness planes. The main assumption is that the failure of claystone material is due to the failure of the rock matrix and the fracturing along weakness planes. For intact matrix: (i) the short-term response includes the main mechanisms (transversely isotropic elastic, hardening, softening and residual plastic strain, brittle-ductile transition) evidenced in laboratory investigations, (ii) the long-term behaviour is based on Lemaître's model in agreement with the laboratory tests. The time-dependent response of weakness planes is described by the Maxwell's model with a threshold. After checking the model on simple stress paths, its operational character is successfully demonstrated on the GCS drift (the more difficult to reproduce the overall observations). The computed convergences (and their ratio) and plastic zone extensions are consistent with the in-situ observations.

Keywords: Constitutive model; Weakness planes, Plasticity, Time-dependent behaviour, M/H-M URL drift.

1 GENERAL LAYOUT

Within the perspective of deep geological radioactive waste disposal, the French National Radioactive Waste Management Agency (Andra) develops research that include in-situ experiments at the Meuse/Haute-Marne Underground Research Laboratory (MHM URL) with the aim to demonstrate the feasibility of constructing and operating a high-level and intermediate-level long-lived waste disposal facility in the Callovo-Oxfordian (COx) claystone formation. Excavation of galleries at the main level of the URL, following essentially the in-situ horizontal principal stress directions (σ_h, σ_H), shows a significant anisotropy of the induced fractured zones, leading to anisotropy of pore pressure distribution and convergence among others (Armand et al. 2014, see Figure 1 for example). Several factors contribute to this anisotropic response: anisotropy of the rock fabric (stiffness, strength), anisotropic in situ stress state, induced pore pressure field, induced quasi-brittle failure, etc.

Over the last 20 years, many experimental tests on samples have been carried out by several European laboratories as part of a continuing effort to better understand and characterize the mechanical, hydromechanical and thermohydromechanical behaviour of COx claystone (Armand et al. 2017) and several constitutive models have been developed.

The present paper is a part of ongoing collaborative scientific research on the development of advanced constitutive models for COx claystone behaviour and robust numerical tools suitable for the numerical modelling in the framework of the Cigéo project. By extending our previous works (Souley et al. 2022), a constitutive model considering the natural and induced anisotropies in the short- and long-term behaviour is proposed. This rheological model for COx claystone consists of an intact matrix with an elastoplastic behaviour where the elasticity is transverse isotropic, and plasticity is isotropic (as a first approach), and an induced anisotropy described by the concept of weakness planes, assumed to occur in the post-peak regime which agrees with tests on samples (Zhang et al. 2019 for example). More precisely, for intact rock matrix: (i) the short-term response incorporates all the main mechanisms evidenced during the laboratory investigations, (ii) the long-term behaviour is based on the isotropic Lemaître's model as suggested by the creep tests carried out on COx samples. A creep threshold is assumed in relation to the observed anisotropy of natural stresses.

The short-term behaviour along the weakness planes is also elastically transverse isotropic and plastically isotropic (Souley et al. 2022) according to Coulomb law. The time-dependent behaviour is simply approximated by the Maxwell's model with a threshold from which the creep starts or stops. The orientation of the weakness planes is based on some evidence of failure in the field of rock mechanics (Jaeger et al. 2007).

The proposed anisotropic model for short and long terms behaviour of COx claystone is then implemented in the finite difference code *FLAC*^{3D}. After checking the mechanical response and the numerical implementation on simple stress paths, its operational character is successfully demonstrated on the experimental GCS drift of MHM URL excavated in the direction of the major horizontal stress with soft support (compressible concrete wedge and shotcrete).

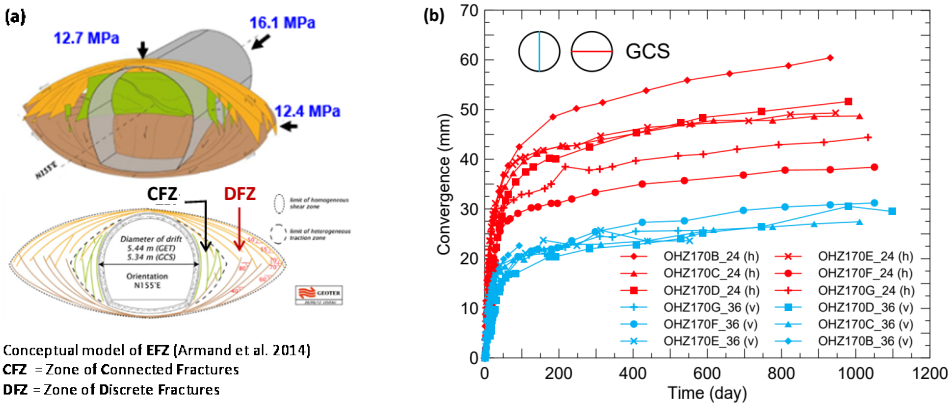

Figure 1. In situ observations around the GCS drift parallel to the major horizontal stress, after Armand et al. (2014). (a) Conceptual model of the induced fractures network around the drift, (b) measured horizontal and vertical convergences.

2 KEY MECHANISMS AND CONSTITUTIVE EQUATIONS

2.1 Constitutive model

As reported by Armand et al. (2017), the key features of the mechanical behaviour of COx claystone can be summarized as follows: (a) a linear elastic and anisotropic behaviour under low deviatoric stresses; (b) a strain hardening approximately at 50% of the peak strength; (c) a brittle failure under low confining pressures, (d) a strain softening for moderate confining pressures; (e) a perfectly plastic behaviour (residual phase) completely frictional and governed by the behaviour of the induced well localized shear bands or macro-cracks (Zhang et al. 2019), (f) the stress-strain curves also showed a

transition between softening and ductile behaviour under high confining stresses. Several constitutive models were proposed to account for most of these mechanisms (Manica et al. 20122, Souley et al. 2022, for example). In Souley et al. (2022), the rock fracturing is modelled by a coupling between weakness planes (viewed as induced damage in post peak regime) and elastoplastic rock matrix. More precisely, the matrix is assumed to be linear elastic, transversely isotropic below the elastic limit and plastic with strain hardening and softening followed by a residual stage. The yield surfaces for the strain hardening and softening are derived from the laboratory characterization and based on the Hoek and Brown criterion expressed in terms of stress invariants (p, q, θ) where the Lode angle θ allows to consider the stresses geometry.

$$F_s{}^m = \frac{4}{3}\frac{cos^2\,\theta}{A}q^2 + \left(\frac{cos\,\theta}{\sqrt{3}} - \frac{sin\,\theta}{3}\right)q + p - \frac{B}{A} \tag{1}$$

where p represents the mean stress, q the generalized deviatoric stress and θ the Lode's angle, A and B are two independent parameters (A=m σ_c and B=s σ_c^2, m and s are Hoek-Brown constants, σ_c is the value of axial stress reached at the initiation and peak under unconfined compressive). During strain hardening and softening, the parameters A and B evolve in a non-linear manner between their elastic limit and the peak strength on the one hand, and the peak and the beginning of the residual stage on the other hand. Finally, according to Souley et al. (2022) a non-associated flow rule is assumed with plastic potential based on Drucker-Prager.

The induced anisotropy (or anisotropic damage) is herein described by weakness planes whose orientation depends on the induced stress distribution. It is assumed that: (a) shear fracture when the principal stress (minor)σ_3 is equal or close to zero with fracture plane oriented normal to σ_3 (i.e., parallel to σ_1-direction) (c) under triaxial compression configuration we consider that the rock fails along conjugate fractures with an angle θ about $\pm(\pi/4 - \varphi_{wp}/2)$ with respect to the direction of σ_1. The weak-plane failure criterion with a tension cut-off is expressed as follow:

$$\begin{cases} F_s{}^{wp} = \tau + \sigma_{nn}\,tan\left(\varphi_{wp}\right) - C_{wp} \\ F_t{}^{wp} = \sigma_{nn} - \sigma_t{}^{wp} \end{cases} \tag{2}$$

where C_{wp}, φ_{wp}, and $\sigma_t{}^{wp}$ are respectively the cohesion, friction angle the tensile strength of the weakness planes. σ_{nn} and τ respectively the normal stress and the generalized shear stress acting on the weakness planes.

The other key characteristic of the behaviour of COx relates to the creep deformations. The time-dependent behaviour of COx is governed by deformation processes corresponding to physical mechanisms at the microstructural level. Creep tests show that the viscoplastic deformation continuously evolves with the applied deviatoric stress and viscoplastic strain rate (Armand et al. 2017). Assuming the existence of a deviatoric stress threshold below which creep does not occur (consistent with the initial anisotropic stress state at the MHM URL), a simplified form of the COx creep behaviour proposed by Souley et al (2017) or Manica et al. (2022), an extension of the Lemaitre's model, is adopted here. The following equation was proposed for the viscoplastic strain tensor rate for the intact (undamaged) rock:

$$\dot{\boldsymbol{\varepsilon}}^{vp} = A_{visc}\,\langle\frac{q - q_0}{\sigma_0}\rangle^n\,{\varepsilon_{eq}}^{vp m_c}\frac{\partial q}{\partial \boldsymbol{\sigma}} \tag{3}$$

where A_{visc} is the viscosity, q_0 the creep threshold, σ_0 the reference stress (typically one stress unit), n a dimensionless exponent corresponding to the deviatoric stress power factor, m_c the exponent of hardening work, $\boldsymbol{\sigma}$ the effective stress tensor, ${\varepsilon_{eq}}^{vp}$ the equivalent deviatoric creep strain, and $\boldsymbol{\varepsilon}^{vp}$ the creep strain tensor.

Creep deformation along a rock discontinuity appears to be depending on whether the fracture is smooth or rough, and whether it is fresh or filled (Malan et al. 1998). For smooth joints, creep is

primarily controlled by an adhesion-friction mechanism. For an unfilled rough joint, creep is due to stress concentrations on the asperities of the joint surfaces, which causes slipping as the asperities progressively failed and the shear stresses redistribute to the other nearby intact asperities (Ladanyi 1993). From the tests of Malan et al. (1998), it was found that the creep deformation, the friction angle and the strength of the tested joints are time dependent. For creep strain, the authors suggest a power law. As we do not have any feedback on the time-dependent behaviour of the weakness planes, we assume a simple model based on the Maxwell's model. This requires only two additional parameters: the shear modulus in the plane of weakness and the viscosity of this same plane.

2.2 Numerical implementation

The proposed constitutive model is implemented into the commercial code *FLAC*^{3D} as a Dynamic Link Library (DLL) file that can be loaded whenever it is needed.

We will not reiterate the verification tests on the short term behaviour widely addressed in Souley et al. (2022) or the discussion concerning the input short term parameters of the matrix also used herein. Thus, only the delayed response will be examined in this exercise of verification.

For the time-dependent behaviour of the intact rock, parameters are those identified from the first series of creep tests performed in 2003 and represent the creep parameters of intact COx claystone. They will be used to simulate a more recent series of creep tests (Armand et al. 2017). The values of the viscosity A_{visc}, the hardening m_c, and the exponent n are respectively: 4.17e-11 h^{-1}, -2.7 and 6.8.

As described in reported by Armand et al. (2017), triaxial compression creep tests of 90 days duration at different deviatoric stresses (q_1=50%, q_2=75% and q_3=90% of the peak strength estimated to be 36.5 MPa), were used to check the numerical prediction. Figure 2 compares the model and the theoretical results of the time evolution of the deviatoric creep strain. A very good agreement is observed (maximum deviation below 0.1%). Figure 2 also compares the evolution of the axial creep strain as a function of time between our simulations and the results of laboratory tests with also a good agreement.

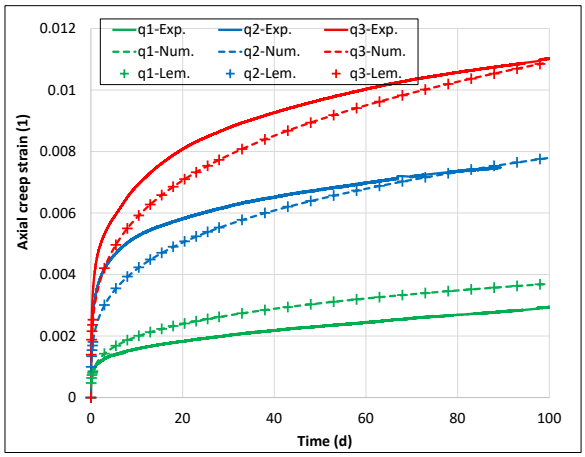

Figure 2. Creep tests on COx claystone: comparison between the model (dashed line), the analytical expression of Lemaitre's model (plus), and results of creep tests of Armand et al. (2017) (solid line).

3 APPLICATION TO THE GCS DRIFT

In addition to the effect of its soft support, the experimental GCS drift (// σ_H = 16.1 MPa) has also been devoted to several instrumentations and in situ measurements (convergences, rock deformation, pore pressure over several years, and specific thermo-hydro-mechanical experiments). The GCS drift remains a challenge for numerical modelling, since to our knowledge, very few authors have successfully proposed a constitutive model of COx claystone behaviour able to properly reproduce most of the in situ observations. Specifically, they are the anisotropies of the EFZ (Extent of Failed

Zone) extension, of the convergences, of the pore pressure distribution, etc., while the initial stress state in the GCS section is quasi-isotropic (σ_v = 12.7 MPa, σ_h = 12.4 MPa). It is also a very interesting case that allows to validate the constitutive models, their numerical implementation and possibly to help in the back-calibration of certain model parameters. For this simulation a viscosity of 5E4 MPa/h was used for the planes of weakness. The shear modulus in the weakness planes is taken equal to that of the bedding plane, i.e., 4000 MPa. Finally, we assume that most instantaneous plastic response was occurred after the full passage of the front (say at 4 diameters, or after 1 month).

The observed EFZ around the GCS drift is illustrated in Figure 1a. The predicted extents of fractured zone (post-peak phase) and plastic zone in pre-peak at the end of excavation, 14 days, 1 month and 2 months after the end of excavation are plotted in Figure 3. The predicted extension of the fractured zones ranging from 0.7 x D to 1 x D at the drift sides is consistent with the observations and the results of 3D numerical short term modelling of GCS (Souley et al. 2022). Moreover, there is practically no evolution of the extent of the failed plastic zones beyond 14 days of creep. This strengthens our assumption on the essentiality of the instantaneous plastic zones/

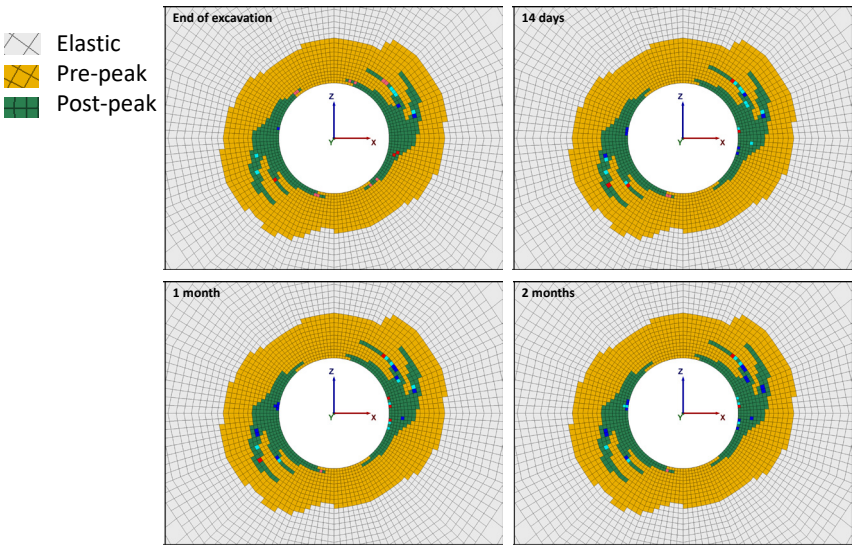

Figure 3. Predicted extent of plastic zones around GCS drift.

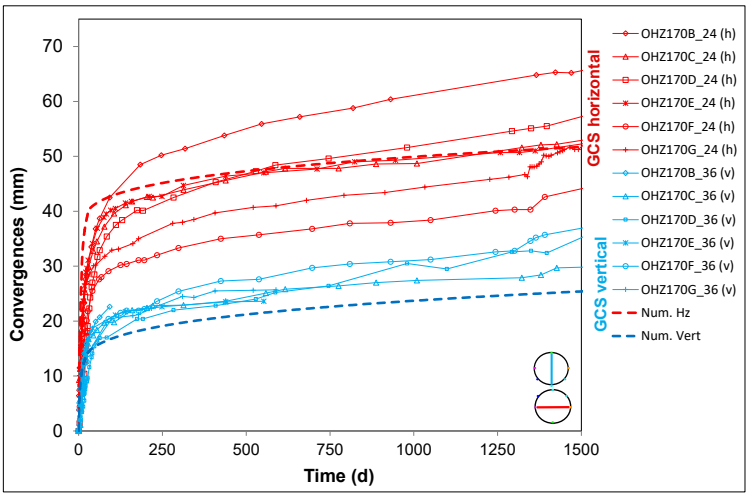

Figure 4. Evolution of horizontal and vertical convergences around the GCS. Comparison between the field measurements and the numerical prediction.

Figure 4 compares the modelled and in situ measured evolution of horizontal and vertical convergences of the GCS drift wall. The strong anisotropic response (which is related to the EFZ

shape) observed in situ is well reproduced by the model. The measured anisotropic convergence has a ratio C_h/C_v ~1.5-2.1, whereas the model results in ratios of 1.3-1.9. The predicted evolution of the horizontal and vertical convergences, as well as their magnitudes are in quite good agreement with in situ measurements.

4 CONCLUSION AND PERSPECTIVE

An anisotropic elastoplastic and viscoplastic model is proposed to describe the short and long terms mechanical behaviour of the COx claystone and implemented in the commercial finite difference code, *FLAC^{3D}*. The main assumption is that the failure of claystone material is due to fracturing along weakness planes (ubiquitous joints) and the failure of the rock matrix. The rock behaviour is characterized by a non-linear behaviour in pre peak, a non-linear softening in post-peak and a perfectly plastic behaviour in the residual phase. The occurrence of the weakness planes and their orientations result from the induced stress state based on the fracture mechanics, which includes tensile, longitudinal splitting and shear cracks. Time-dependent behaviour of both the intact claystone matrix and the weakness planes (induced anisotropy) is considered in the proposed model. After checking the numerical implementation on creep test paths, its operational character is successfully demonstrated on the GCS drift (parallel to σ_H: the more difficult to reproduce the overall observations).

It is well known that modelling of geomaterials exhibiting a strain-softening behaviour with continuous approaches leads to numerical solutions heavily dependent on the size of the mesh elements and sometimes to numerical instabilities. The perspective will be to regularize this model with for instance an implicit gradient method, based on the Helmholtz differential equation.

REFERENCES

Armand, G., Conil, N., Talandier, J. & Seyedi, D.M. 2017. Fundamental aspects of the hydromechanical behaviour of Callovo-Oxfordian claystone: from experimental studies to model calibration and validation. *Computers and Geotechnics* 85:277-286

Armand, G., Leveau, F., Nussbaum, C., de La Vaissiere, R., Noiret, A., Jaeggi, D., Landrein, P. & Righini, C. 2014. Geometry and properties of the excavation induced fractures at the Meuse/Haute-Marne URL drifts. *Rock Mechanics and Rock Engineering* 47(1):21–41. doi:10.1007/s00603-012-0339-6

Jaeger, J.C, Cook NGW. & Zimmerman RW. 2007. Fundamentals of rock mechanics, 4th edn. Blackwell Publishing, Oxford, p 475

Ladanyi, B. 1993. Time-dependent response of rock around tunnels. In: Fairhurst C (ed). *Comprehensive rock engineering: principles, practice & projects.* Vol. 2, Analysis and design methods. Oxford: Pergamon, pp 77–112

Malan, D.F., Drescher, K. & Vogler, U.W. 1998. Shear creep of discontinuities in hard rock surrounding deep excavations. In: Rossmanith H-P (ed). Mechanics of jointed and faulted rock: *proceedings of the third International Conference on Mechanics of Jointed and Faulted Rock – MJFR*-3, Vienna, Austria, 6–9 April 1998. Rotterdam : Balkema, pp 473–478

Mánica, M.A, Gens, A., Vaunat, J., Armand, G. & Vu, M.N. 2022. Numerical simulation of underground excavations in an indurated clay using non-local regularisation. Part 1: Formulation and base case. *Geotechnique*, 72(12):1092–112

Souley, M., Armand, G. & Kazmierczak, J-B. 2017. Hydro-elasto-viscoplastic modeling of a drift at the Meuse/Haute-Marne underground research laboratory (URL). *Computers and Geotechnics* 85 (2017) 306–320

Souley, M., Vu, M.N. & Armand, G. 2022. 3D Modelling of Excavation-Induced Anisotropic Responses of Deep Drifts at the Meuse/Haute-Marne URL. *Rock Mechanics and Rock Engineering,* doi.org/10.1007/s00603-022-02841-

Zhang, C-L., Armand, G., Conil, N. & Laurich, B. 2019. Investigation on anisotropy of mechanical properties of Callovo-Oxfordian claystone. *Engineering Geology* 251 (2019) 128–145